A semivariance-based index for spatially correlated errors in rapid differential GNSS applications

Narve Schipper Kjorsvik

Abstract In this work, a regional network of permanent Global Navigation Satellite Systems (GNSS) receivers is used to estimate the decorrelation of the spatially correlated errors in differential GNSS positioning. Emphasis is laid on the dispersive errors (i.e. mainly the ionosphere). A new index, based on variance as function of station separation (semivariance) is proposed and compared to the existing I95 index. This study uses data from the 29–30th October 2003, a period with severe ionospheric activity. The proposed index is shown to give realistic predictions of differential measurement accuracy, and has potential for further development towards use in RTK-networks.

Introduction

Errors affecting positioning with Global Navigation Satellite Systems (GNSS) are often divided into station specific errors and spatially correlated errors. Station specific errors include, e.g. multipath and measurement noise. Spatially correlated errors include, e.g., ionospheric delay, tropospheric delay and ephemeris errors.
The impact of spatially correlated errors is greatly reduced using differential methods, provided the inter-station separation is "sufficiently small". The maximum allowable separation is thus both application dependent and dependent on the magnitudes of the underlying errors.

Received: 19 May 2004 / Accepted: 11 August 2004
Published online: 4 September 2004

N. S. Kjorsvik
Department of Mathematical Sciences and Technology,
Agricultural University of Norway, P.O. BOX 5003,
1432 Aas, Norway
E-mail: narve.kjorsvik@imt.nlh.no
Tel.: +47-64-948842
Fax: +47-64-948810

In rapid or instantaneous differential positioning aiming at centimeter-level accuracy, an important prerequisite is the correct determination of the double-differenced carrier phase integer ambiguities. Reliable ambiguity resolution is seriously hampered when systematic errors caused by significant differential errors are present, as is the case with large ionospheric gradients. Large differential errors will thus make real-time differential positioning difficult, and they have the potential to severely degrade the accuracy of the computed coordinates.
A special study group of the International Association of Geodesy (IAG) working with "Quality Issues in Real-Time GPS Positioning" stated in its report (Rizos 1999) that "quality control [...] related to systematic error mitigation and stochastic modelling" is one of the crucial issues. The report also stated that very few objective quality measures existed.
In a single-baseline set-up, it is difficult to separate the various errors from the baseline components. A permanent network of reference stations is, however, well suited for this purpose, and the service provider can routinely produce and broadcast statistics on the past and currently expected measurement conditions for GNSS users operating within or in the vicinity of the network.
Wanninger (1999) proposed the I95 index as a measure of the impact of ionospheric refraction on rapid positioning. The I95 index is the 95 percentile of the double-differenced ionospheric gradients in a triangle of reference stations. The 95 percentiles must be computed over some samples to be representative, e.g. 1 h or day, thus making instantaneous measures difficult.
More recent contributions include Chen et al. (2003), in which they discuss a linearity indicator for the ionosphere. This indicator is computed by omitting one of the reference stations and then comparing its measurements with the interpolated values. The RMS of the residuals are then accumulated over 1 h and used as an indicator of linearity. The linearity indicator may provide valuable information if the linear part is modelled and removed, as in Network RTK (e.g. Wanninger 1995), but gives no relation to measurement conditions as a function of baseline length. Leaving out one station also implies that the station spacing increases, possibly leading to non-linear behaviour of the differential ionosphere.
Accuracy of the computed coordinates follows from the usual relation

$$\sigma_x = \sigma_0 \mathrm{DOP} \quad (1)$$

where σ_x is the position accuracy (standard deviation), DOP is the geometric dilution of precision, and σ_0 is the measurement accuracy. A common practice (e.g. Schaffrin and Bock 1988) is to divide the measurement accuracy into a constant and a distance dependent part:

$$\sigma_0^2 = a^2 + b^2 D^2 \tag{2}$$

where a is a constant (units of distance), b is a constant (unit-less) and D is the station separation. The constant a is a lower bound for observation accuracy due to receiver and site specific effects, typically in the range of 5–10 mm for double-differenced carrier phase observations. The constant b reflects the decorrelation of the spatially correlated errors with increasing station separation, typically in the range of a few parts per million (ppm).
In the following section, we will start with Eq. 2 and develop an index based on variance as function of station separation (semivariance) rather than on the actual gradients as is the case with the I95 index.

Semivariance

In the following, we will define the semivariance and comment on some special considerations and assumptions in relation to the new index. The semivariance is defined for an intrinsically stationary process $f(u)$ as (Christensen 2001, Chapter 6.1)

$$\gamma(u,v) = \gamma(u-v) = \frac{1}{2}\mathrm{Var}(f(u) - f(v)). \tag{3}$$

Thus, the semivariance of an intrinsically stationary process is not a function of the positions of two stations but a function of the baseline between them. An intrinsically stationary process is isotropic if

$$\gamma(u-v) = \gamma(\|u-v\|). \tag{4}$$

Related to the development of the new index, this implies that the semivariance is a function of baseline length only, and not baseline orientation. Assuming an isotropic semivariance function, it can be estimated by (Christensen 2001, Chapter 6.8)

$$\hat{\gamma}(\|h\|) = \frac{1}{2N_h}\sum_{i=1}^{N_h}(f_i - f_{i(\|h\|)})^2 \tag{5}$$

where $(f_i - f_{i(\|h\|)})$, i=1,…, N_h are N_h pairs of data separated by the distance $\|h\|$.
There are several ways to estimate parameters in a functional fit of a semivariance function to the data at hand. In the following section, we will use a least squares adjustment.

A proposed index

We propose the following approach to compute an index for the impact of spatially correlated errors on differential positioning:

1. Obtain representative values for the constant part of the observation accuracy (parameter a) for the network in use.
2. Resolve double-differenced carrier phase ambiguities between the reference stations in the network.
3. Compute measurement residuals using fixed ambiguities on a common level, i.e. relative to a common reference station and reference satellite.
4. Compute semivariances for each epoch and satellite in all linearly independent station pair combinations for the dispersive and non-dispersive parts of the residuals separately.
5. Estimate the slope of a straight line (parameter b of Eq. 2) through the square root of the semivariances, using the a priori value of parameter a.
6. Compute the indices at each epoch, or to represent the conditions over a limited time span (e.g. 1 min, 1 h or 1 day) by moving averages or 95 percentiles.

The constant part of the observation accuracy is primarily a function of hardware design and the surroundings of the antenna. This leads to the assumption that this parameter is stable over a long period. In a homogenous network with fairly identical hardware set-ups, it should be possible to condense the information into an average statistic. This accuracy estimate should be obtained from long-term estimation and averaging, and not included in the epoch-wise estimation.
Semivariance is computed using Eq. 5 applied independently on each baseline formed from all linearly independent station pair combinations. Related to Eq. 5 this means f_i denotes measurement residuals for satellite i and N_h denotes number of satellites.
We propose to fit the line using a least squares estimation process. A problem can arise when the estimated slope (b) turns out to be negative, as this has no physical meaning in this context. This situation will arise from time to time when working with real data, as a linear model is a clear simplification. We therefore suggest that any negative slopes are assigned the value zero.

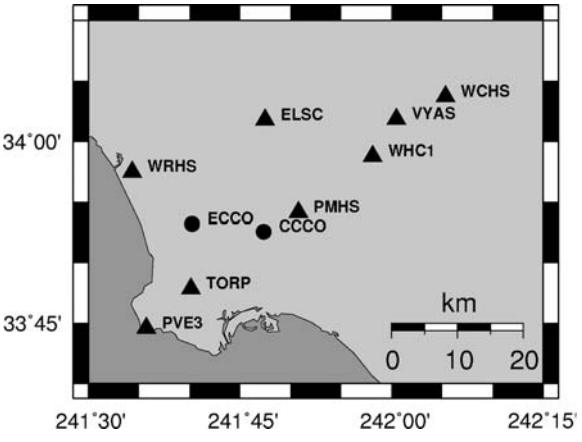

Fig. 1
Map showing a part of the SCIGN. Stations used as references are marked with *triangles*, while stations serving as "user stations" are marked with *circles*

Implementation

A network solution was computed using the in-house software *gps_net_init*, described in e.g. Kjorsvik et al. (2003). This multi-purpose tool was extended with semi-variance estimation capabilities and computation of the I95 index.

In this context, station coordinates are considered as known quantities, and thus the carrier phase ambiguities remain as the sole unknowns in the system of equations. Ambiguities are determined by first identifying the optimal set of independent baselines based on an iterative algorithm described in Mervart (1995). In this study, the optimality criteria was chosen to be the shortest possible baseline.

The ambiguity determination follows a classical wide lane/narrow lane approach (see e.g. Mervart 1995) and a sequential least squares search. All data are used in each iteration and parameters are estimated in a least squares batch. The highest visible satellite common to all stations is always chosen as reference satellite. This strategy is expected to minimize the double-differenced residuals, as the impact of both the ionosphere and the troposphere tend to grow with decreased elevation. Hence, this strategy will also ease the initial ambiguity resolution in the

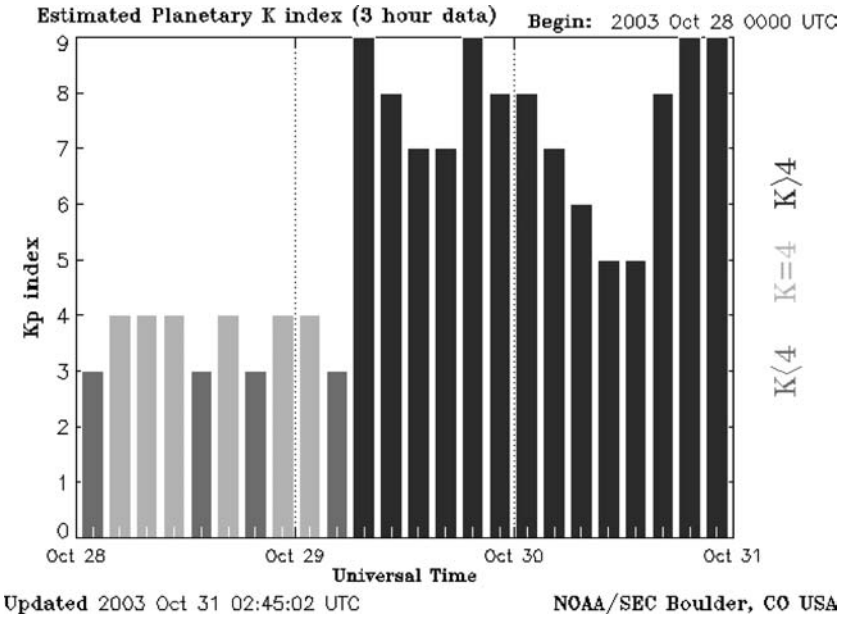

Fig. 2
Planetary Kp-index. (Figure courtesy of NOAA/SEC, Boulder, CO, USA)

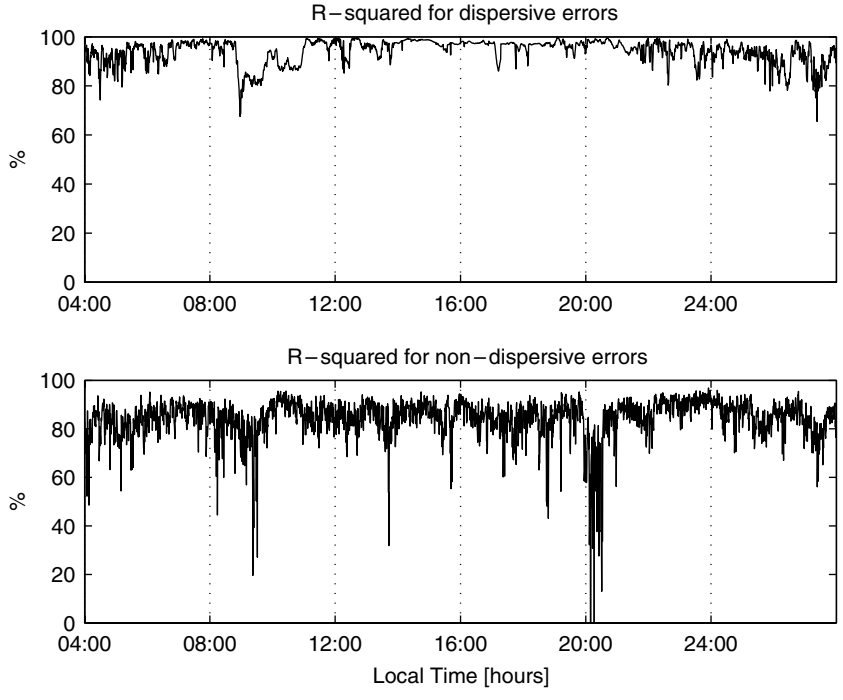

Fig. 3
R^2 values after fitting a linear model to the estimated semivariances; for the dispersive part (*top*) and non-dispersive part (*bottom*)

network. Elevation cut-off was set to 15° throughout this study.

Cycle slips are detected using triple-differences and discontinuities in the single-differenced ionospheric residuals. No attempt is made to repair the cycle slips, rather the program is instructed to introduce new ambiguity parameters. No outlier detection is performed on the carrier phase observations, but only phase arcs with more than 10 min continuous observations are included in the ambiguity resolution. Ambiguities are validated using the *W* ratio (Dai et al. 2003) and a threshold of 3 (corresponding to a confidence level of 99.9%). In addition, ambiguities are discarded if the round off value exceeded 0.4 cycles. Observations with floating ambiguities are excluded from further analysis.

Observations are corrected for tropospheric delay using the Saastamoinen model (Saastamoinen 1973) and Niell mapping functions (Niell 1996) with a standard atmosphere, i.e. a pressure of 1013.25 hPa, a temperature of 18 °C and a relative humidity of 60%. The dispersive (I) and the non-dispersive (T) parts of the carrier phase residuals are separated using the formulas

$$I = -\frac{\bar{\varphi}_1 - \bar{\varphi}_2}{1 - (f_1^2/f_2^2)} \tag{6}$$

$$T = \bar{\varphi}_1 + I, \tag{7}$$

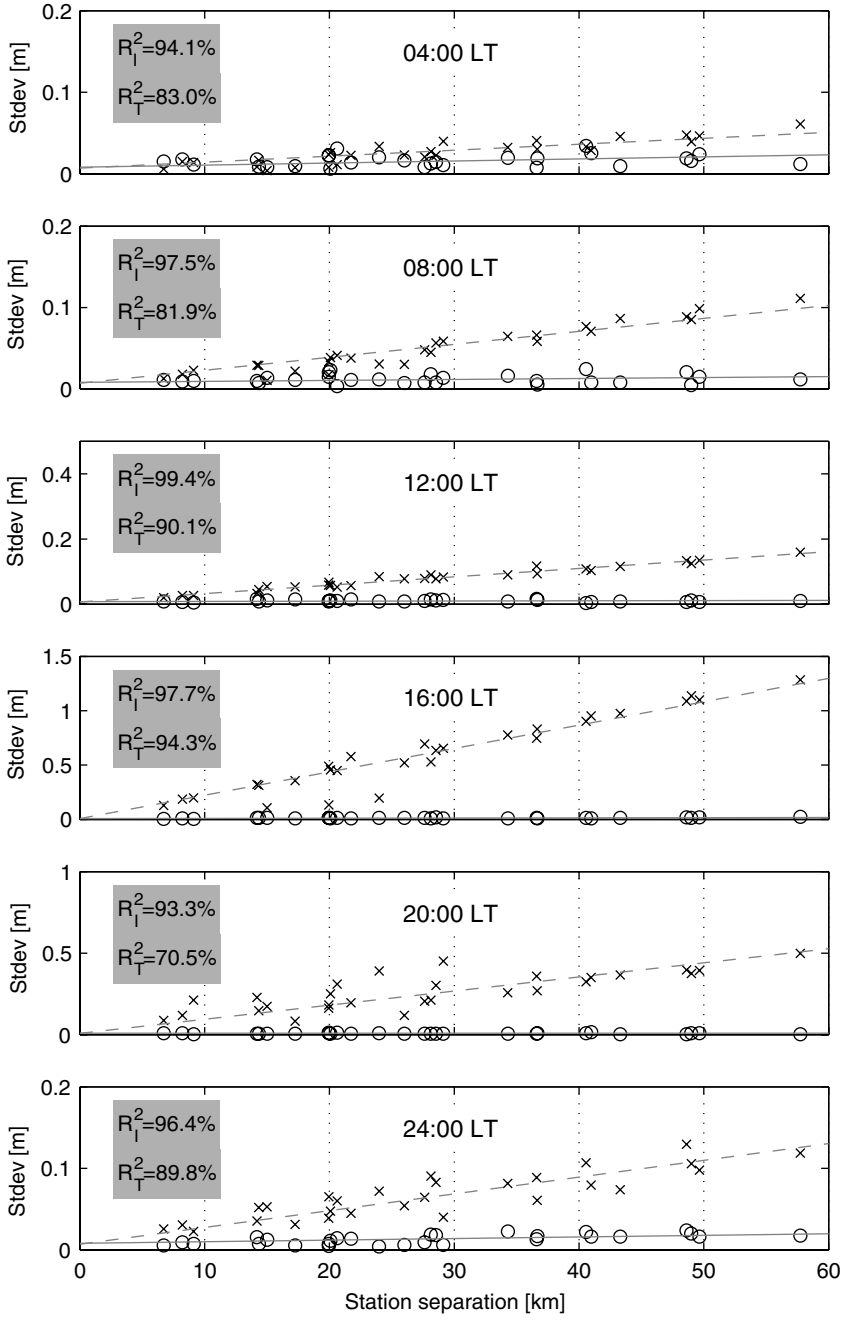

Fig. 4
Linearity of the square root of the sample semivariance estimates at six epochs. *Crosses* and *circles* denote dispersive and non-dispersive parts, respectively, with the fits shown as *lines*

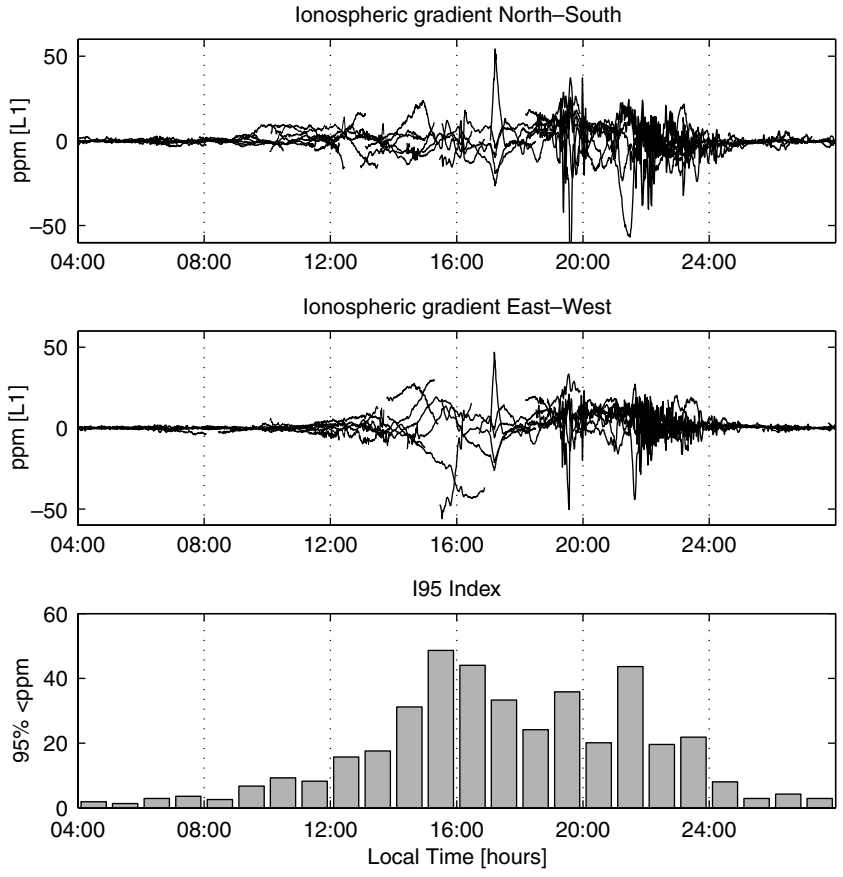

Fig. 5
Ionospheric gradients (*top* North-South, *middle* East-West) and corresponding hourly I95 indices (*bottom*)

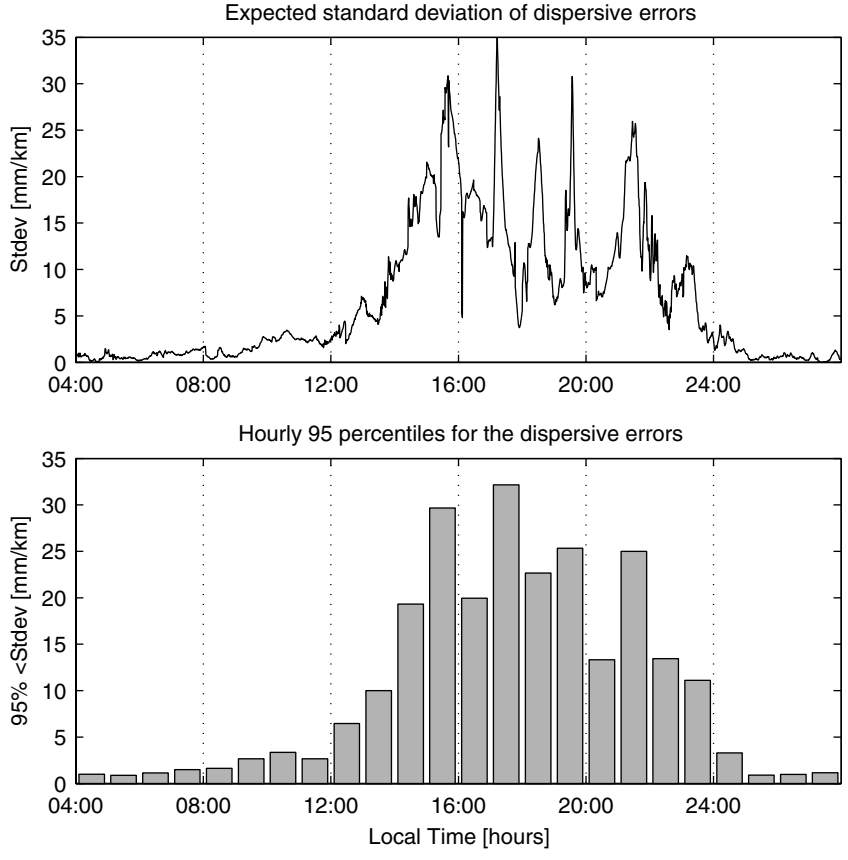

Fig. 6
The proposed index computed for the dispersive errors using all reference stations. The *upper plot* shows epoch-by-epoch estimates, and the *lower* shows corresponding hourly 95 percentiles

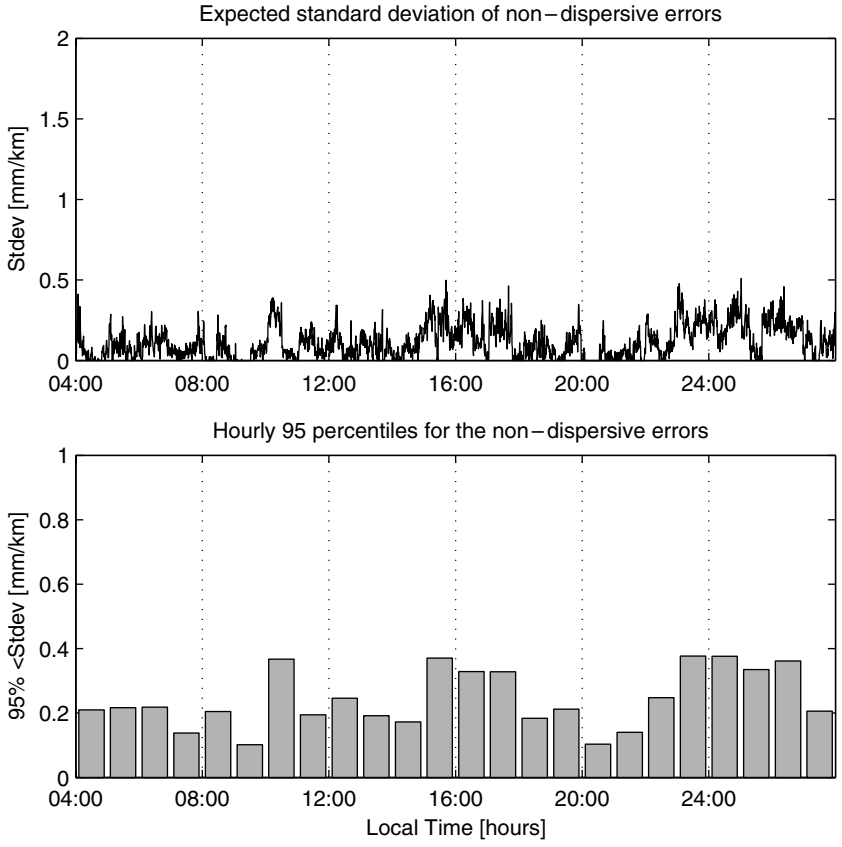

Fig. 7
The proposed index computed for the non-dispersive errors using all reference stations. The *upper plot* shows epoch-by-epoch estimates, and the *lower* shows corresponding hourly 95 percentiles

where $\bar{\varphi}$ denotes the carrier phase residuals, subscripts 1 and 2 and the terms f_1 and f_2 indicate L1 and L2 frequencies.

Empirical results

A subset of ten stations of the Southern California Integrated GPS Network (SCIGN) was chosen for this test. Eight of the stations served as reference stations, while two stations served as "user stations" (see Fig. 1). All sites were equipped with Ashtech Z-XII receivers with various chokering antennas. Relative antenna calibrations from the National Geodetic Survey (Mader 1999) were therefore employed to minimize the effect of using different antennae.

Data from this network, as well as others, are freely available through the Internet (Scharber et al. 2004). This web interface also gives access to a database of daily coordinate solutions in the ITRF2000 reference frame. Two full days of observation data sampled at 30 s were downloaded and merged into 24 h files starting at 12.00 UT (04.00 Local time (LT)) on the 29 October 2003. Coordinate solutions for the 29th of October were downloaded and considered valid for both days. Final precise ephemerides from the International GPS Service (IGS) were used.

Using the rather conservative ambiguity resolution and validation strategy described above, approximately 99.2% of the carrier phase observations had their corresponding ambiguities successfully determined.

The earth was subject to extreme geomagnetic activity during parts of these days due to major coronal mass ejections on the sun (see, e.g. Schaer 2003). The planetary Kp index is a measure of the global geomagnetic activity. Indices for this dataset are shown in Fig. 2, and indicate geomagnetic storms over periods of this dataset.

The constant term of the observation accuracy (parameter a of Eq. 2) was not estimated in this study, as this would require processing of several weeks of data. Instead, it was derived from a priori assumptions. Reasonable estimates of accuracy of undifferenced carrier phase observations would be 1 mm for L1 and 2 mm for L2 in terms of standard deviation. When propagating these through Eqs. 6 and 7 and using a factor 2 when considering double-differenced observations, this leads to standard deviations of 7 mm for the dispersive signals and 8 mm for the non-dispersive signals. Erroneous values may have some impact on the computed index for non-dispersive errors due to their relative small magnitudes. The ionosphere dominates differential dispersive errors; hence, it is not likely that a slightly erroneous value for the constant part will have any effect on the index.

We define R^2 as

$$R^2 = 1 - \frac{e^T e}{Y^T Y} \tag{8}$$

where e denotes the residuals from fitting a model through the observations Y. That is, R^2 describes the proportion of

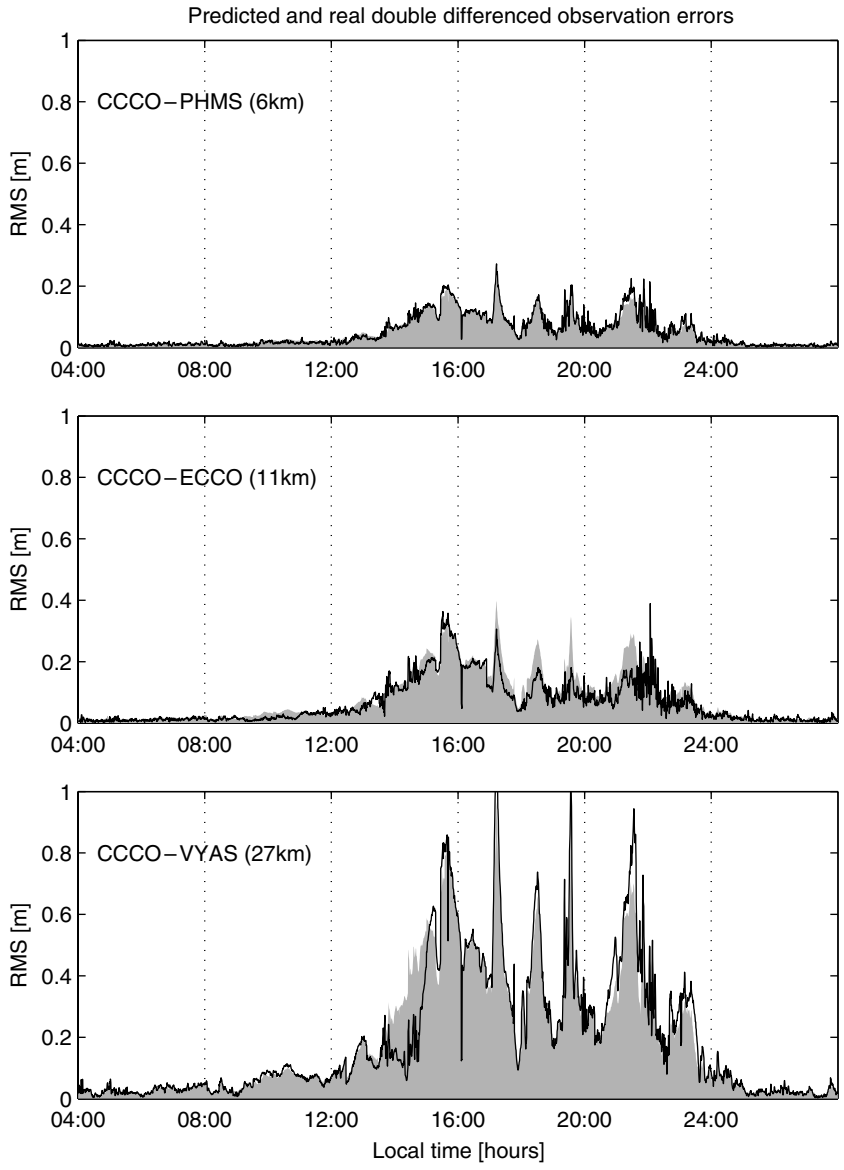

Fig. 8
Dispersive parts of the predicted (*shaded greys*) and real (*solid lines*) RMS of the double-differenced observation residuals for three "user baselines"

the information (in terms of sum of squares) explained by fitting a model, with large values (close to unity) indicating a good fit. In this context, e denotes the residuals after a least squares fit of a linear model (Eq. 2) and the observations Y are the estimated semivariances (by Eq. 5) of the dispersive or non-dispersive errors derived by Eqs. 6 and 7.

As a first verification of the concept and to verify the adequacy of a linear model, R^2 values were computed at each epoch for both the dispersive and non-dispersive parts as shown in Fig. 3. In addition, snapshots of semivariance estimates were plotted from 04.00 to 00.00 LT in 4-h steps as shown in Fig. 4. To enhance the readability, the square root of the semivariance is plotted and should thus be linear with station separation.

The dependence between variance and baseline length is reflected in the high R^2 values (around 90%) for the dispersive parts. The R^2 values are generally lower for the non-dispersive parts (around 80%), but with a few spikes to around 20% and even to slightly negative values around 20.00 LT. The latter is an extreme case where using the model is actually worse than assuming no model at all. All these cases with low R^2 values (poor fits) are associated with negative slopes being truncated to zeros (see Fig. 7), i.e. cases with poor signal to noise ratios.

The plots show that the assumptions are reasonably well fulfilled throughout this data set, both regarding the magnitude and constant nature of parameter a and regarding the linear relationship between accuracy and baseline length (parameter b).

Figure 5 shows the estimated ionospheric gradients using a data rate of 30 s and the corresponding hourly I95 indices using three reference stations in the perimeter of the network (PVE3, ELSC and WCHS).

Figures 6 and 7 show the results using the proposed index for the same data set. The Kp index ranges from 7 (04.00 LT) through 8 and 9 (morning and noon) and finally

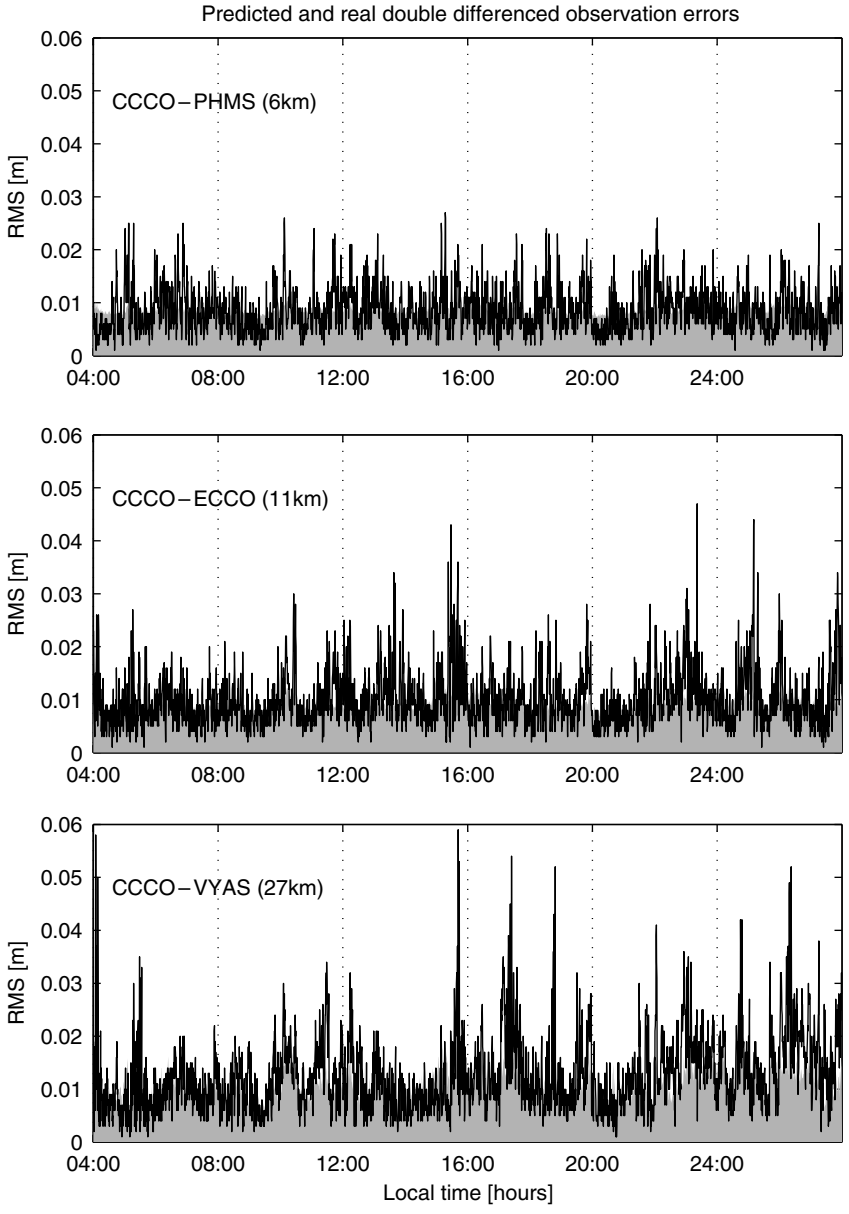

Fig. 9
Non-dispersive parts of the predicted (*shaded greys*) and real (*solid lines*) RMS of the double-differenced observation residuals for three "user baselines"

declines to 5 through the night. This indicates a major storm event. Both the I95 index and the new index show that the impact on differential positioning is small in the morning on the 29th, but reaching extreme values from local noon. A single satellite can be seen to reach a peak gradient of approximately 80 ppm at 19.00.

In this dataset and network and by using precise ephemeris, the signals of the non-dispersive errors seem to be just above the noise level, i.e. the Saastamoinen troposphere model and Niell mapping functions with a standard atmosphere almost completely eliminate the troposphere. The applicability of the index to predict measurement accuracy is verified by computing some "user-baselines" within the network. These baselines are processed using the same strategy and settings as for the reference stations, i.e. using 24 h of data and fixed station coordinates.

Double differenced measurement residuals are formed for various baselines between the "user-stations" (ECCO and CCCO) and some of the reference stations. RMS of the double-differenced measurement residuals are shown in Figs. 8 and 9 together with the predicted values according to the proposed index. The predicted accuracies show a very good agreement for all three baselines throughout the dataset, including the extreme ionospheric storm periods. Some spikes can be observed in the bottom two plots of Fig. 9, showing the RMS of the real double-differenced non-dispersive observations. This could have several explanations; such as observation outliers or higher order ionospheric effects not accounted for by Eqs. 6 and 7.

Summary and outlook

We have proposed an index that can be used to predict the performance of differential positioning. Although a very

high correlation can be seen between the proposed index and the I95 index, the proposed index has the advantage of having a clear relation to anticipated measurement accuracy and is thus easier to interpret.

Although precise ephemerides were used in this study, broadcast or predicted ephemerides (e.g. from IGS) can be used, thus allowing (near) real-time capabilities.

The index is suitable for all spatially correlated errors, e.g. separate indices may be computed for the dispersive and non-dispersive errors, or they may be lumped together in an overall index. Indices may be computed at each epoch or, e.g. on an hourly basis using 95 percentiles.

The proposed index seems to perform well even under an extreme ionospheric storm, and provides realistic predictions of the measurement accuracy.

A quadratic growth of the variances is obviously not realistic when the network size increases dramatically, rather, some asymptotical behaviour can be expected. A quadratic growth of variance is, however, a fair assumption in regional networks of a few hundreds of kilometers.

The functional fit of the semivariance function should be further investigated. It is possible that a more sophisticated method than least squares could be applied.

The method could be further developed to allow the index to be computed in the context of RTK networks, i.e. to quantify the quality of the broadcast corrections (or Virtual Reference Station data). This information can be used to further enhance ambiguity resolution for user baselines by, e.g. applying a locally optimized "weighted ionosphere" approach.

It should be investigated if the semivariance function should be made anisotropic. This may be a more correct assumption in case of, e.g. travelling ionospheric disturbances or at latitudes where ionospheric conditions are dominated by gradients in one direction.

The variance of the non-dispersive signals is obviously height dependent, as well as dependent on the spherical distance, and this should probably be reflected in the semivariance model.

Acknowledgements We acknowledge the Southern California Integrated GPS Network and its sponsors, the W.M. Keck Foundation, NASA, NSF, USGS and SCEC, for providing data used in this study. The author wishes to thank the reviewers for their useful comments and criticism.

References

Chen X, Landau H, Vollath U (2003) New tools for network RTK integrity monitoring. In: Proceedings of ION GPS/GNSS 2003, Portland. The Institute of Navigation, pp 1355–1360

Christensen R (2001) Advanced linear modelling. Springer texts in statistics, 2nd edn. Springer, Berlin Heidelberg New York

Dai L, Wang J, Rizos C, Han S (2003) Predicting atmospheric biases for real-time ambiguity resolution in GPS/GLONASS reference station networks. J Geodesy 76(11–12):617–628

Kjorsvik N, Ovstedal O, Svendsen JGG, Blankenberg LE (2003) Evaluation of a multi-base station differential approach. In: Proceedings of ION GPS/GNSS, Portland. The Institute of Navigation, pp 1381–1389

Mader GL (1999) GPS antenna calibration at the national geodetic survey. GPS Solutions 3(1):50–58

Mervart L (1995) Ambiguity resolution techniques in geodetic and geodynamic applications of the Global Positioning System. PhD Thesis, University of Berne

Niell AE (1996) Global mapping functions for the atmosphere delay at radio wavelengths. J Geophys Res 101(B2):3227–3246

Rizos C (1999) Quality issues in real-time GPS positioning. Report from Special Study Group 1.154. International Association of Geodesy—Travaux 1999

Saastamoinen J (1973) Contributions to the theory of atmospheric refraction. Bulletin Géodésique 107(1):13–34

Schaer S (2003) Exceptionally high TEC levels on days 302 and 303. IGSMAIL-4683. http://igscb.jpl.nasa.gov/mail/igsmail2003/msg00459.html

Schaffrin B, Bock Y (1988) A unified scheme for processing GPS dual-band phase observations. Bulletin Géodésique 62:142–160

Scharber M, Bock Y, Gilmore B (2004) Software tools for accessing the GPS Seamless Archive. GPS Solutions 7(4):271–274

Wanninger L (1995) Enhancing differential GPS using regional ionospheric error models. Bulletin Géodésique 69(4):283–291

Wanninger L (1999) The performance of virtual reference stations in active geodetic GPS-networks under solar maximum conditions. In: Proceedings of ION GPS 1999, Salt Lake City. The Institute of Navigation, pp 1419–1427